SMALL-CRACK GROWTH AND FATIGUE-LIFE PREDICTION OF CORRODED OPEN-HOLE SPECIMENS

J. C. Newman, Jr.[1] & W. Abbott[2]
[1]Department of Aerospace Engineering, Mississippi State University, Mississippi State, MS, USA 39762
[2]Battelle Memorial Laboratory, Columbus, OH 43201

ABSTRACT

This paper uses small-crack theory and a plasticity-induced crack-closure model to predict the fatigue lives of 2024-T3 aluminum alloy sheet specimens with open holes subjected to either remote tension or cantilever bending loads. The tension specimens were pristine laboratory specimens that had a drilled and polished hole; whereas, the bending specimens had three drilled holes that were either pristine or exposed to outside weather conditions at various locations for 3 to 12 months. The exposed specimens developed various levels of corrosion pits in and around the holes. These pre-corroded specimens were then returned to the laboratory and fatigue tested under laboratory-air conditions with cantilever bending loads.

The present paper uses fatigue-crack growth with an equivalent-initial-flaw-size (EIFS) to fit the fatigue behavior of these specimens. Crack-growth-rate data on small and large cracks were used to develop the effective stress-intensity factor range (ΔK_{eff}) against crack-growth rate relation for the material. Crack-tip constraint factors, to account for state-of-stress effects, were selected to correlate large-crack data over a wide range in stress ratios and stress levels under constant-amplitude loading. Some modifications to the ΔK_{eff}-rate relation were needed in the near-threshold regime to fit measured small-crack-growth-rate behavior, ignoring large-crack data in the near threshold regime. The model was then used to calculate small- and large-crack-growth rates, and to predict total fatigue lives, for notched specimens under constant-amplitude loading for pristine and corroded conditions. Fatigue lives were calculated using the crack-growth-rate relation and micro-structural features (like inclusion particle and corrosion-pit sizes) that initiated cracks in the aluminum alloy specimens. The EIFS values, needed to fit the fatigue behavior, agreed well with the median corrosion-pit size measured on the corroded specimens. Small-crack theory and the plasticity-induced crack-closure model with corrosion-pit sizes, like those measured, were able to calculate the fatigue lives quite well.

1 INTRODUCTION

On the basis of linear-elastic fracture mechanics (LEFM), studies on small fatigue cracks (10 μm to 1 mm) have shown that these cracks grow much faster than large-crack behavior and grow below the large-crack threshold [1]. However, the small-crack data were compared with large-crack data generated using a load-reduction procedure. It is suspected that the load-reduction procedure is inducing inappropriately low rates and high thresholds due to a rise in the crack-closure level [2] that may be due to a load-history effect, such as remote closure [3]. Thus, the large-crack behavior may be the anonymous behavior and small-crack growth may indeed be the appropriate results. Over the past twenty years, various studies on small- or short-crack growth behavior in metallic materials [4-6] have led to the realization that fatigue life of many materials is primarily "crack growth" from micro-structural features, such as inclusion particles, voids or slip-band formation. Concurrently, improved fracture-mechanics analyses of some of the crack-tip shielding mechanisms, such as plasticity-induced crack closure, and analyses of surface- or corner-crack configurations have led to more accurate crack growth and fatigue-life prediction methods. “Small-crack theory” is the treatment of fatigue as a crack-propagation process from a micro-structural discontinuity (or crack) to failure. Fatigue and fracture mechanics concepts have merged to form a unified treatment of the fatigue process for many engineering materials [7].

The objective of this paper is to use small-crack theory and a plasticity-induced crack-closure model [8,9] to calculate fatigue lives of 2024-T3 aluminum alloy sheet specimens with open holes subjected to either tension or cantilever bending loads. The tension specimens were pristine specimens that had a drilled and polished hole; whereas, the bending specimens had three drilled holes that were either pristine or exposed to outside weather conditions at various locations

for 3 to 12 months. The exposed specimens developed various levels of corrosion pits in and around the holes. These pre-corroded specimens were then returned to the laboratory and fatigue tested under laboratory-air conditions with cantilever bending loads.

Fatigue of these specimens was treated as a purely fatigue-crack-growth process from micro-structural features (like inclusion particle or corrosion-pit sizes) that initiated cracks at the holes in the aluminum alloy. The equivalent-initial-flaw-size (EIFS) values, needed to fit the fatigue behavior, are compared with corrosion-pit depths measured on the corroded specimens. A relation between the EIFS values and the measured corrosion-pit depths was developed. A methodology is proposed to predict the fatigue behavior of exposed specimens using measure corrosion-pit sizes.

2 MATERIAL AND SPECIMEN CONFIGURATIONS

Fatigue-crack-growth data on 2024-T3 aluminum alloy sheet (B = 2.3 mm) were obtained from middle-crack-tension, M(T), specimens [10-12] that ranged from 76 to 305 mm wide. The specimens were tested over a wide range in stress ratio and stress levels. The yield stress (σ_{ys}) and ultimate tensile strength (σ_u) of the aluminum alloy were 360 and 490 MPa, respectively.

Two types of fatigue test results were analyzed: (1) open-hole specimens subjected to remote tension and (2) specimens with three holes subjected to cantilever bending. Fatigue tests were conducted on 50.8-mm wide specimens under tension with a 3.18-mm diameter circular hole that had been drilled and polished [13]. Tests were conducted at both R = 0 and -1.

Fatigue tests were also conducted on specimens that had three open holes and were subjected to cantilever bending, see Figure 1. Loads were applied to the specimen to cause bending fatigue failures at the hole closest to the support. These data have been obtained from Bill Abbott, Battelle Memorial Laboratories (unpublished data). The fatigue data generated by Battelle is a series of three-hole specimens that have been exposed at various U.S. Air Force Bases (Wright-Patterson, Daytona, etc.) for 3, 6, 9 and 12 months; and specimens that had not been exposed. After exposure, the specimens were returned to Battelle and fatigue tested. Pit-size distributions on the exposed specimens were also measured.

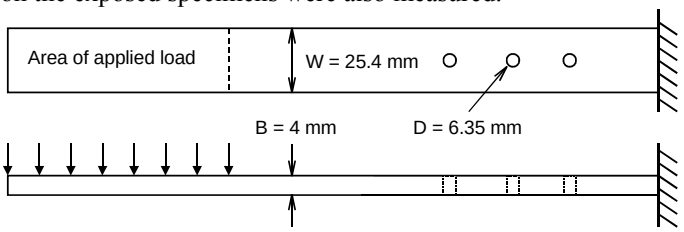

Figure 1: Cantilever bending coupon with three holes.

To make fatigue-life and crack-growth predictions, ΔK_{eff} as a function of crack-growth rate must be obtained over a wide range in rates (from threshold to fracture). Under constant-amplitude loading, the only unknown in the crack-closure analysis is the constraint factor, α. The constraint factor was determined by finding (trial-and-error) a value (or values) that will correlate the crack-growth-rate data over a wide range in stress ratios [9].

3 SMALL- AND LARGE-FATIGUE-CRACK-GROWTH RATES

Large-crack results for 2024-T3 aluminum alloy are shown in Figure 2 for data generated by Hudson [10], Phillips [11] and Dubensky [12]. This figure shows the elastic ΔK_{eff} plotted against crack-growth rate. The data collapsed into a narrow band, except for some large differences in the high-rate regime. These tests were conducted at very high remote stress levels (0.75 to 0.95 of the yield stress). The elastic-plastic fracture criterion (Two-Parameter Fracture Criterion, see Ref. 14) used in the analysis (K_F = 267 MPa$\sqrt{m}$; m = 1) predicted failure very near to the vertical

asymptotes of these test data, see vertical lines for R = 0.7 and 0.5. Lower R ratios would fail at higher values of ΔK_{eff}. For these calculations, a constraint factor (α) of 2.0 was used for rates less than 1E-07 m/cycle and α = 1.0 was used for rates greater than 2.5E-06 m/cycle. For intermediate rates, α was varied linearly with the logarithm of crack-growth rate. Values of α and rate were selected by trial-and-error (see Ref. 15). The constraint-loss regime (α = 2 to 1) has also been associated with the flat-to-slant crack-growth behavior. An expression to predict the location of the flat-to-slant crack-growth regime and the effective stress-intensity factor at transition is by

$$(\Delta K_{eff})_T = 0.5\ \sigma_o\ \sqrt{B} \qquad (1)$$

where σ_o is the flow stress of the material (average between σ_{ys} and σ_u).

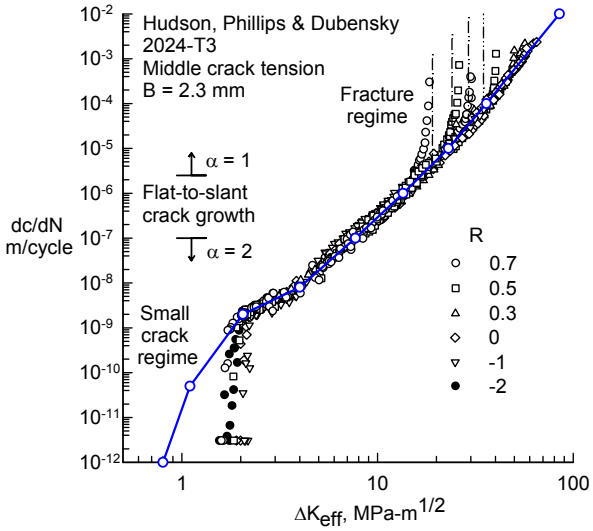

Figure 2: Effective stress-intensity factor for 2024-T3 aluminum alloy sheet material.

For the 2024-T3 alloy, $(\Delta K_{eff})_T$ = 10.2 MPa$\sqrt{m}$. The width of the constraint-loss regime, in terms of rate or ΔK_{eff}, is a function of thickness (B), but this relation has yet to be developed. In the low crack-growth rate regime, near and at threshold, tests and analyses [2,3] have indicated that the threshold may be too high due to load-history effects. In the threshold regime, the actual ΔK_{eff} -rate data would lie at lower values of ΔK_{eff}. For the present study, an estimate was made on the basis of small-crack data [4] and is shown by the solid line below 2E-09 m/cycle. The baseline relation shown by the solid line (and open circles) was used to predict fatigue lives under constant-amplitude loading for both corroded and non-corroded specimens.

4 FATIGUE-LIFE PREDICTIONS

Small-crack theory -- a total fatigue-life prediction methodology based solely on crack propagation from micro-structural features (or corrosion pits) will be used to predict fatigue life on the non-corroded and corroded specimens. In this approach, a crack is assumed to initiate and grow from a micro-structural feature (or a corrosion pit) on the first cycle. The crack-closure model and the baseline ΔK_{eff}-rate curve were used to predict crack growth from the initial crack size to failure. The final crack size was calculated from the fracture toughness of the material. Comparisons are made with fatigue tests conducted on circular-hole specimens subjected to remote tension or cantilever bending that have been exposed or not exposed to harsh environments.

4.1 Laboratory Specimens

Figure 3 shows fatigue tests on laboratory specimens under remote tension (Fig. 3a) and cantilever bending (Fig. 3b). The curves are the calculated results from small-crack theory for various EIFS values.

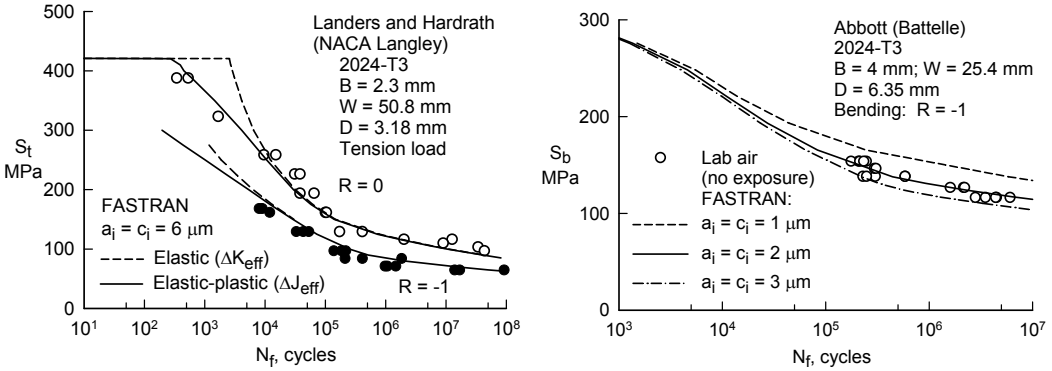

(a) Remote tension specimens (b) Cantilever bending specimens

Figure 3: Measured and calculated fatigue tests on laboratory specimens (no exposure).

Landers and Hardrath [13] determined fatigue lives on the aluminum alloy with a central hole (Fig. 3a). The predicted results, as shown by the curves, were made using an initial semi-circular crack size (6 μm) that had an equal area to the average inclusion-particle sizes that initiated cracks [4]. Results from the elastic-plastic analyses agreed fairly well with the test data, but the elastic analyses over-predicted fatigue lives at the high stress levels. The influence of stress ratio on fatigue limits was also predicted quite well using a value of $(\Delta K_{eff})_{th}$ of 0.8 MPa√m (determined from un-notched specimens [16]). The smaller initial crack size for a notched specimen compared to that for un-notched specimen (20 μm) [16] is probably due to a much smaller volume of material under the stress that caused failure.

Stress levels reported on the specimens with three open holes and subjected to cantilever bending were measured with a strain gage located mid-way between the critical hole and the free edge. Due to the stress concentration of the hole, the stress levels were expected to be higher than the outer fiber bending stresses, S_b, used in the stress-intensity factor solutions for a corner crack at a hole. Private communication with Abbott indicated that specimens with and without holes produced stress levels that were 15.1 to 17.7% higher in the open-hole coupon than in the no-hole coupon. Thus, the stress levels reported in the Battelle work has been reduced by 16.4%.

Figure 3(b) shows a comparison of measured and calculated fatigue lives on some of the 3-hole specimens that have not been exposed to a harsh environment, but prepared and tested under laboratory-air conditions. S_b is the remote outer fiber bending stress and N_f is the cycles to failure. The solid symbols show the test data from Abbott (Battelle) and the curves were calculated from FASTRAN using three different initial crack sizes. The 2-μm initial corner flaw fit the S-N behavior quite well. These results also demonstrate that at a low applied stress level the calculated fatigue lives show a large scatter from 1 to 3-μm initial corner flaws, whereas at higher applied stress levels very little difference occurred for these same flaw sizes.

4.2 Exposed and Corroded Specimens

Figure 4 shows the results of fatigue tests conducted on three-hole specimens under bending that have been exposed to outdoor environments at two U. S. Air Force Bases. The curves are the calculated results from small-crack theory for various EIFS values to fit these test data.

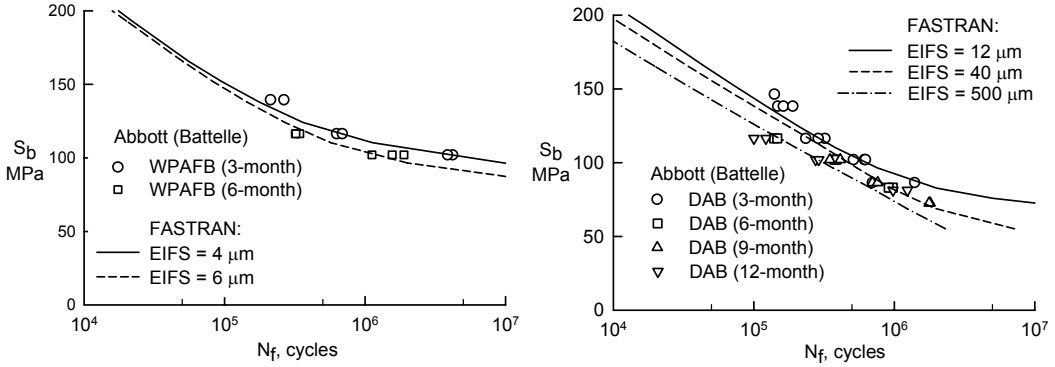

(a) Wright-Patterson Air Force Base (b) Daytona Air Force Base

Figure 4: Measured and calculated fatigue lives on exposed specimens.

Figures 4a and 4b show the results of fatigue tests conducted on exposed 3-hole specimens under R = -1 remote bending loads. The specimens were exposed for 3 to 12 months at the respective U.S. Air Force Bases, removed and returned to Battelle, and then fatigue tested in a laboratory-air environment until failure. FASTRAN was then used to find an EIFS to fit the test data. In the analysis, a small corner crack at the edge of the open hole was considered as the initial defect. The ΔK_{eff}-rate relation for cracks growing in laboratory air was used in the crack-growth analysis. The EIFS values were found to be larger at Daytona AFB than at the Wright-Patterson AFB; and EIFS values were larger for more exposure time at both bases.

Exposed specimens were examined before testing to measure the pit depth, d; and the cumulative distribution function for pit depths at the two U.S. Air Force Bases are shown in Figure 5a. Pit depths were larger at the Daytona AFB than at the Wright-Patterson AFB; and pit depths were larger for more exposure time at both bases.

Noting that there appeared to be a direct relationship between the pit depths and the EIFS values used to fit the fatigue tests, Figure 5b shows a plot of the EIFS values against the 50-percentile value from Figure 5b. The dashed line is perfect agreement and the solid curve shows an approximate upper-bound fit to these data. With the exception of one data point, there appeared to be a one-to-one relationship. In other words, the pit depth may be considered the EIFS in life calculations.

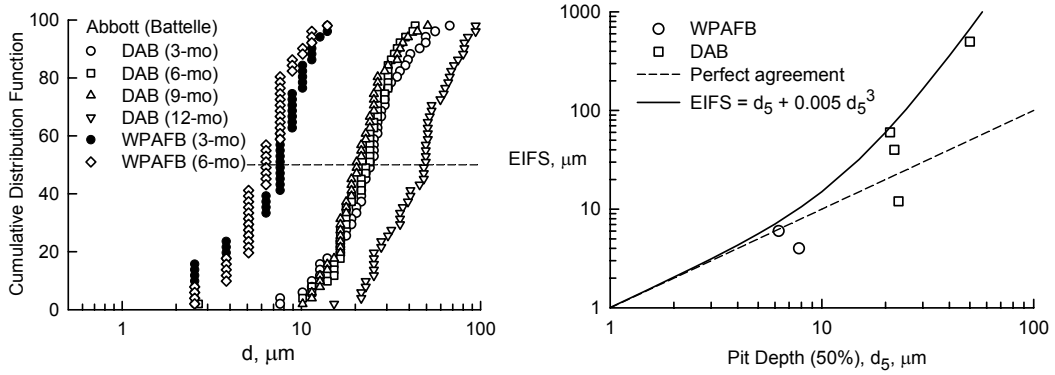

(a) Corrosion-pit depth distributions (b) Relation between EIFS and pit size.

Figure 5: Comparison between corrosion-pit-size distributions and EIFS for two airbases.

5 CONCLUDING REMARKS

Small-crack theory and a plasticity-induced crack-closure model (FASTRAN) have been used with an equivalent-initial-flaw-size (EIFS) concept to fit the fatigue (S-N) behavior on 2024-T3 aluminum alloy specimens subjected to remote tension or cantilever bending loads. One group of specimens had pristine drilled and polished holes subjected to remote tension, while the other specimens had three holes and were exposed to outside weather conditions at various U. S. Air Force bases. The exposed specimens developed various stages of corrosion pitting, which influenced the subsequent fatigue lives. Using the EIFS values to fit the S-N behavior, a nearly linear relationship was obtained between the measured corrosion-pit depths and the calculated EIFS values. The life-prediction methodology presented may be used to assess the influence of corrosion pitting on structural lives of aircraft exposed at the various locations.

6 REFERENCES

1. Pearson S. (1975) Initiation of fatigue cracks in commercial aluminum alloys and the subsequent propagation of very short cracks. Engng Fract Mech, 7(2):235-247.
2. Minakawa K and McEvily AJ. (1981) On near-threshold fatigue crack growth in steels and aluminum alloys. Proc Int Conf Fatigue Thresholds, 2:373-390.
3. Newman Jr JC. (1983) A nonlinear fracture mechanics approach to the growth of small cracks. AGARD CP 328:6.1-6.26.
4. Newman Jr JC and Edwards PR. (1988) Short-crack growth behaviour in an aluminum alloy – AGARD cooperative test programme. AGARD R-732.
5. Short-crack growth behaviour in various aircraft materials. (1990) Edwards PR and Newman Jr JC (eds.), AGARD R-767.
6. Newman Jr JC, Wu XR, Venneri S and Li CG. (1994) Small-crack effects in high-strength aluminum alloys – NASA/CAE cooperative program. NASA RP-1309.
7. Newman Jr JC. (1997) The merging of fatigue and fracture mechanics concepts: a historical perspective. ASTM STP 1321:3-51.
8. Newman Jr JC. (1981) A crack-closure model for predicting fatigue crack growth under aircraft spectrum loading. ASTM STP 748:53-84.
9. Newman Jr JC. (1992) FASTRAN II - A fatigue crack growth structural analysis program. NASA TM-104159.
10. Hudson CM. (1969) Effect of stress ratio on fatigue-crack growth in 7075-T6 and 2024-T3 aluminum alloy specimens. NASA TN D 5390.
11. Phillips EP. (1988) The influence of crack closure on fatigue crack growth thresholds in 2024-T3 aluminum Alloy . ASTM STP 982:505-515.
12. Dubensky RG. (1971) Fatigue crack propagation in 2024-T3 and 7075-T6 aluminum aAlloys at high stress. NASA CR 1732.
13. Landers CB and Hardrath HF. (1956) Results of axial-load fatigue tests on electropolished 2024-T3 and 7075-T6 aluminum alloy sheet specimens with central holes. NACA TN 3631.
14. Newman Jr JC. (1976) Fracture analysis of various cracked configurations in sheet and plate materials. ASTM STP 605:104-123.
15. Newman Jr JC. (1992) Effects of constraint on crack growth under aircraft spectrum loading. Fatigue of Aircraft Materials, Beukers et al (eds), Delft University Press, 83-109.
16. Newman Jr JC. (1994) Review of modeling small-crack behavior and fatigue-life prediction for aluminum alloys. Fat Frac Engng Mat Struct. 17:429-439.